

# 1 Hydrological response in the Danube lower basin to some 2 internal and external climate forcing factors

5 Ileana Mares<sup>1</sup>, Venera Dobrica<sup>1</sup>, C. Demetrescu<sup>1</sup>, C. Mares<sup>2</sup>

7 <sup>1</sup> Institute of Geodynamics, Romanian Academy, Bucharest, Romania

8 <sup>2</sup> National Institute of Hydrology and Water Management, Bucharest, Romania

12 **Abstract.** Of the internal factors, we tested the predictors from the fields of  
13 precipitation, temperature, pressure and geopotential at 500hPa. From the external factors, we  
14 considered the indices of solar/geomagnetic activity. Our analysis was achieved separately for  
15 each season, for two time periods 1901-2000 and 1948-2000.

16 We applied developments in empirical orthogonal functions (EOFs), cross  
17 correlations, power spectra, filters, composite maps. In analysis of the correlative results, we  
18 took into account, the serial correlation of time series.

19 For the atmospheric variables simultaneously, the most significant results (confidence  
20 levels of 95%) are related to the predictors, considering the difference between standardized  
21 temperatures and precipitation (TPP), except for winter season, when the best predictors are  
22 the first principal component (PC1) of the precipitation field and the Greenland-Balkan-  
23 Oscillation index (GBOI). The GBOI is better predictor for precipitation, in comparison with  
24 North Atlantic Oscillation index (NAOI) for the middle and lower Danube basin.

25 The significant results, with the confidence level more than 95%, were obtained for  
26 the PC1-precipitation and TPP during winter/spring, which can be considered good predictors  
27 for spring/summer discharge in the Danube lower basin.

28 Simultaneous, the significant signal of geomagnetic index (aa), was obtained for the  
29 smoothed data by band pass filter. For the different lags, the atmospheric variables respond to  
30 solar/geomagnetic activity after about 2-3 years. The external signals in the terrestrial  
31 variables are revealed also by power spectra and composite maps. The power spectra for the  
32 terrestrial variables show significant peaks that can be associated with the interannual  
33 variability, Quasi-Biennial Oscillation influence and solar/geomagnetic signals.

34 The filtering procedures led to improvement of the correlative analyses between solar  
35 or geomagnetic activity and terrestrial variables, under the condition of a rigorous test of the  
36 statistical significance.

37 **Keywords:** NAO, GBOI, serial correlation, low and band pass filter, atmospheric blocking,  
38 Danube basin, climate changes

## 41 1 Introduction

43 Climatic system is a closed system, being influenced mainly by external factors,  
44 whose action is modulated by the internal mechanisms. Therefore, it is difficult to assess  
45 climatic system response to various external factors, the discrimination action of each is  
46 sometimes even impossible. The main external factors as is known are: solar activity in its  
47 various forms and the greenhouse gases that cause climate variability. The quantifying the

48 impact of each factor on the climate system is subject to various ~~uncertainties~~ 49 ~~uncertainties~~. As shown in 50 Cubasch et al. (1997) as well as in Benestad and Schmidt (2009) is difficult to distinguish 51 between anthropogenic signal and the solar forcing in the climate system, especially if we 52 wanted to assess if the greenhouse or the solar forcing ~~could be responsible for~~ 53 ~~responsible for~~ the recent 54 warming. An explanation of this shortcoming is related to the ~~limits~~ of simulation climate 55 models and lack of long data on many parts of the Earth, to estimate the impact of solar 56 activity.

57 In Brugnara et al. (2013) are reviewed recent studies on the impact of solar activity / 58 geomagnetism on the climate. After a statistical reconstruction of the main atmospheric fields 59 for more than 250 years, the authors performed an analysis of the solar signal of 11 years in 60 different terrestrial datasets, and they found that there was a robust response of the 61 tropospheric late-wintertime circulation to the sunspot cycle, independently from the ~~data set~~. 62 This response is particularly significant over Europe.

63 There were many preoccupations regarding the impact of greenhouse gases, resulting 64 from climate modeling under various scenarios, on the water regime of the Danube. We 65 mention only some of these studies. In Mares et al. (2011, 2012) were processed climate 66 variables obtained from four global models of climate change: CNRM, ECHAM5, EGMAM 67 and IPSL, under A1B scenario. It was found for Danube lower basin, that the probability to 68 have extreme events (hydrological drought and great discharges) increases in the second half 69 of the 21<sup>st</sup> century comparing to the first half. A more complex methodology for post- 70 processing of outputs of climate model is found in Papadimitriou et al. (2016), where an 71 analysis of the changes in future drought ~~ontology~~ was performed for five major European 72 basins (including Danube) and the impact global warming was estimated.

73 Regarding internal factors that influence climate at regional or local scale, best known 74 index is related to the North Atlantic Oscillation (NAO). After Hurrell et al. (2003), NAO is 75 an internal variability mode of the atmosphere that depends exclusively on the dipolar 76 pressure distribution.

77 For the south - eastern European zone, only NAO is not a good enough predictor for 78 Danube discharge. Rimbu et al. (2002) showed that there is an out-of-phase relationship 79 between the time series of the Danube river discharge anomalies and the NAO. Also, 80 Rimbu et al. (2005) was found that spring Danube discharge anomalies are 81 ~~significantly~~ 82 ~~significantly~~ related to winter Sea Surface Temperature (SST) anomalies. In Mares et al. (2002) was found 83 that NAO signal in climate events in the Danube lower basin is relatively weak, in 84 comparison with other regions.

85 However, we must note that NAO is a very good predictor for some regions. Thus, for 86 example NAOI is a significant predictor for : Seine river (Massey et al., 2010; El - Janyani et 87 al., 2012), northeastern Algeria (Turki, et al., 2016), southern Sweden (Drobyshev et al., 88 2011), the northern Italy (Zanchettin et al., 2008).

89 The recent research (Valty et al., 2015) warns that for the predictor's selection such as 90 NAO, need to consider the dynamics of the total oceanic and hydrological system over wider 91 areas. In fact all climate system needs to be considered. In Hertig et al. (2015) are described 92 the mechanisms underlying the non-linearity and non-stationarity of the climate system 93 components, with a focus on NAO and the consequences of climate non-stationarities are 94 discussed.

95 In the present study, in comparison with the NAO influence on climate variables in the 96 Danube basin, we analysed the atmospheric index Greenland-Balkan-Oscillation (GBO), 97 which reflect the baric contrast between the Balkan zone and the Greenland zone. The GBO 98 index was introduced first time in Mares et al. (2013b) and in the present study it is shown in 99 detail, the GBOI informativity in comparison with NAOI, for the Danube basin.

97 Taking into account that solar activity plays an essential role in modulating the  
 98 **blocking parameters** with the strongest signal in the Atlantic sector (Barriopedro et al., 2008;  
 99 Rimbu and Lohmann, 2011), in the present paper we consider also, the indices of atmospheric  
 100 circulation of blocking type.

101 In this paper, except for the highlighting the atmospheric circulation of blocking type  
 102 taking into account the Quasi-Biennial Oscillation (QBO) phases and solar minimum or  
 103 maximum (number Wolf), we did not investigate any further interaction between internal and  
 104 external factors. This interaction was developed in other papers such as Van Loon and Meehl  
 105 (2014).

106 The main aim of our work was to select predictors from the terrestrial and solar  
 107 /geomagnetic variables with a significant informativity for predictand, i.e. discharge in the  
 108 Danube lower basin. We obtained this informativity by applying robust tests for the statistical  
 109 significance. Because the solar and geomagnetic variables, as well as the smoothing  
 110 procedures through various filters, respectively low pass filter and band pass filters applied in  
 111 this investigation, shows strong serial correlations, all correlative analyzes were performed  
 112 through rigorous testing of statistical significance. The number of observations was reduced to  
 113 the effective number of degrees of freedom, corresponding to the independent observations.

114 This paper is organized as follows: Sect. 2 shows data processed at regional scale (2.1)  
 115 and large scale (2.2), as well as the indices that define solar and geomagnetic activity (2.3).

116 In Section 3, we describe the methodology used. There are many investigations related  
 117 to solar / geomagnetic signal in the Earth's climate, some of them use smoothing of data, both  
 118 related to solar activity and the terrestrial variables. This smoothing induces a high serial  
 119 correlation, which produces very high correlations between time series ~~analysis~~. Some authors  
 120 investigating these signals in the terrestrial variables take into account these large serial  
 121 correlations induced by these smoothing, others do not. Therefore in Sect. 3 we focused on  
 122 testing the statistical significance of solar / geomagnetic signal in climate variables, taking  
 123 into account the high autocorrelation induced by the smoothing processes. ~~The confidence~~  
 124 ~~level is found by robust method~~. We also briefly described the procedure of testing of  
 125 confidence levels of the peaks of the power ~~spectra~~.

126 Section 4 contains the results and their discussion. Concerning ~~link~~ between  
 127 atmospheric circulation at the large scale and the climate variables at local ~~and~~ regional scales  
 128 and described in 4.1, we demonstrated that GBOI is a ~~predictor~~ **more significant** than NAOI  
 129 for the climate variables in the Danube middle and lower basin. In 4.2, for the period 1901-  
 130 2000, we considered several predictors depending on climatic variables in the Danube basin,  
 131 as well the indices of large-scale atmospheric circulation and we tested predictor's weight for  
 132 the discharge in the lower basin. In subsection 4.3, are presented the results obtained from the  
 133 analysis of solar/geomagnetic signal simultaneously with the terrestrial variables (4.3.1) and  
 134 with some lags (4.3.2) and QBO role in modulating these signals (4.3.3). The conclusions are  
 135 presented in the Sect.5.

136  
 137

## 138 2 Data

### 139 2. 1 Regional scale

140 Since the Danube discharge estimation has great importance for the economic sector  
 141 of Romania, in the present investigation we focused on predictors for Danube lower basin  
 142 discharge. The lower basin Danube discharge was evidenced by **Orsova station (Q\_ORS)**,  
 143 located at the entrance of the Danube in Romania and representing an integrator of the upper  
 144 and middle basin. Our analysis was achieved separately for each season, for the two time  
 145

146

147 periods 1901-2000 and 1948-2000. For the period 1901-2000 in the Danube upper and  
 148 middle basin (DUMB), were considered fields of precipitation (PP), mean temperature (T),  
 149 diurnal temperature range (DTR), maximum and minimum temperatures (Tmx, Tmn), cloud  
 150 cover (CLD) at 15 meteorological stations upstream of Orsova. The selection of stations was  
 151 done according to their position on the Danube or on the tributaries of the river (Fig.1). The  
 152 values of monthly precipitation and temperature (CRU TS3.10.01) accessing  
 153 (<http://climexp.knmi.nl>). Data-sets are calculated on high-resolution (0.5 x 0.5 degree) grids  
 154 by Climatic Research Unit (CRU), and selected for each station (with the respective  
 155 co-ordinates) the option "half grid points".  
 156 The stations position in relation to Orsova is given in Figure 1. For each station was  
 157 calculated a simple drought index (TPPI), which is calculated by the difference between  
 158 standardized temperatures and precipitation. All analyses were achieved using the seasonal  
 159 averages for all variables considered in this study.

## 160 161 2.2 Large scale

162 In order to see the influence of large-scale atmospheric circulation on the variables  
 163 on the regional scale, we considered the seasonal mean values of sea level pressure field (SLP)  
 164 on the sector ( $50^{\circ}\text{W}$ - $40^{\circ}\text{E}$ ,  $30^{\circ}$ - $65^{\circ}\text{N}$ ). We had to extract SLP data from the National Center  
 165 for Atmospheric Research (NCAR), (<http://rda.ucar.edu/datasets/ds010.1>). As mentioned in  
 166 the associated documentation, this dataset contains the longest continuous time series of  
 167 monthly gridded Northern Hemisphere sea-level pressure data in the DSS archive. The 5-  
 168 degree latitude/longitude grids, computed from the daily grids, begin in 1899 and cover the  
 169 Northern Hemisphere from  $15^{\circ}\text{N}$  to the North Pole. The accuracy and quality of this data is  
 170 discussed in Trenberth and Paolino (1980).  
 171

172 We found a new index started from tests achieved using correlative analysis between  
 173 the first principal component (PC1) of the Empirical Orthogonal Functions (EOF) of the  
 174 development of the precipitation field defined at 15 stations from Danube basin and each grid  
 175 point where SLP is defined. By determining the centers of inverse correlation nuclei (positive  
 176 and negative) and by considering the normalized differences between SLP at Nuuk and Novi  
 177 Sad (Fig.2), we obtained this index, which we called *Greenland-Balkan-Oscillation index*  
 178 (GBOI). This index was introduced by Mares et al. (2013b) and tested in the previous works  
 179 of the authors (Mares et al., 2014a, 2015a,b, Mares et al., 2016a,b).  
 180 The NAOI were derived from <http://www.ledo.columbia.edu/res/pi/NAO/>

181 For 1948-2000, beside of variables taken over 1901-2000, we considered and  
 182 blocking type indices.

183 For the geopotential at 500 hPa (1948-2000) provided by *British Atmospheric Data  
 184 Centre (BADC)* three sectors were taken into account: Atlantic-European (AE) on the domain  
 185 ( $50^{\circ}\text{W}$ - $40^{\circ}\text{E}$ ;  $35^{\circ}\text{N}$  -  $65^{\circ}\text{N}$ ), Atlantic (A) defined in ( $50^{\circ}\text{W}$  -  $0^{\circ}$ ,  $35^{\circ}\text{N}$  -  $65^{\circ}\text{N}$ ) and European  
 186 (E) in the region ( $0^{\circ}$  -  $40^{\circ}\text{E}$ ;  $35^{\circ}\text{N}$  -  $65^{\circ}\text{N}$ ).  
 187

## 188 2.3 Solar / geomagnetic data

189 For this 100 year period the solar/geomagnetic activities were quantified by Wolf  
 190 number and *aa* index. For the period 1948-2000, solar forcing is quantified by the 10.7 cm  
 191 solar flux instead of Wolf number. Since the 10.7cm flux is a more objective measurement,  
 192 and always measured on the same instruments, this proxy "sunspot number" should have a  
 193 similar behaviour but smaller intrinsic scatter than the true sunspot number  
 194 ([ftp://ftp.ngdc.noaa.gov/STP/SOLAR DATA/](ftp://ftp.ngdc.noaa.gov/STP/SOLAR_DATA/)). The values for the Quasi-Biennial Oscillation  
 195

197 (QBO) were downloaded from Free University of Berlin (<http://www.geo.fu-berlin.de/met/ag/strat/produkte/qbo/qbo.dat>).

199

### 200 3 Methodology

202 The time series of the variables considered in the 15 stations **were filtered by the first**  
 203 **principal component** (PC1) of empirical orthogonal functions (EOFs) development.

204 The **analyse** of the low frequency components of the atmosphere, based on  
 205 decomposition in multivariate EOF (MEOF), was used by the author in the present paper in  
 206 Mares et al. (2009, 2015, 2016a, b).

207 The 500 hPa geopotential field **was filtered by blocking index** ( $I_B$ ) as is described in  
 208 Lejenas and Okland (1983). Such a blocking event can be identified when the averaged zonal  
 209 index computed as the 500-hPa height difference between  $40^\circ$  and  $60^\circ\text{N}$ , is negative over  $30^\circ$   
 210 in longitude. Taking into account the above definition, in the present study, we calculated for  
 211 each longitude  $\lambda$ , three indices for the regions: Atlantic-European (AEBI), Atlantic (ABI) and  
 212 Europe (EBI) after the formula:

$$213 \quad 214 \quad IB(\lambda) = \Phi(\lambda, 57.50\text{ N}) - \Phi(\lambda, 37.50\text{ N}) \quad (1)$$

215 where  $\Phi$  is the 500 hPa geopotential field, and blocking index  $I_B$  is a mean for  $\lambda$  longitudes of  
 216  $IB(\lambda)$ . In our case  $IB$  positive reflects a blocking type circulation.

217 In the preprocessing analyses, low and band pass filters were applied.

218 **Low pass filters were** applied to eliminate oscillations due to other factors as El  
 219 Niño–Southern Oscillation (ENSO) than the possible influence of solar/ geomagnetic  
 220 activities. The Mann filter (Mann, 2004, 2008) was applied with three variants that eliminate  
 221 frequencies corresponding **the** periods lower than 8, 10 and 20

222 Besides the low pass filters specified above, which **was** applied only to the terrestrial  
 223 fields, **the band pass filters** were applied **both** to the terrestrial and solar or geomagnetic  
 224 variables. The band pass filters were of the Butterworth type, and the variables have been  
 225 filtered in the 4-8, 9–15 and 17-28 years bands.

226 In Lohmann et al. (2004) the solar variations associated with the Schwabe, Hale, and  
 227 Gleissberg cycles were detected in the spatial patterns in sea-surface temperature and sea-  
 228 level pressure, using band pass filters with frequencies appropriate to each of the solar cycles.  
 229 Significant correlations between global surface air temperature and solar activity were  
 230 obtained by Echer et al. (2009), applying wavelet decomposition **with different the band**  
 231 **frequencies**.

232 As is known in the literature, the response of climate variables to the  
 233 **solar/geomagnetic activity is evidenced not only simultaneously but also certain differences**,  
 234 **we performed cross - correlation with a lag of 5 years**. Explanation of the physical mechanism  
 235 of correlations with certain lags between solar activity and climate variables is found in Gray  
 236 et al. (2013) and Scaife et al. (2013).

237 In order to find the significance level of the correlation coefficient, we have to take  
 238 into account the fact that by the smoothing both terrestrial and solar/ geomagnetic variables  
 239 present a serial correlation. In this case, we have to estimate the equivalent sample size (ESS).  
 240 There are more methods to find the correlations statistical significance among the series pairs  
 241 presenting serial correlations. A part of these methods are present in Thiebaut and Zwiers  
 242 (1984), Zwiers and Storch (1995), Ebisuzaki (1997).

243 In Mares et al. (2013a), the procedure described by Zwiers and Storch (1995) for ESS  
 244 estimation was applied in order to estimate the statistical significance of the climatic signal in  
 245 sea level pressure field (SLP) in 21<sup>st</sup> century in comparison with 20-th century.

247 In the present analysis, in order to find the ESS, namely the *number* of *effectively* independent  
 248 observations ( $N_{\text{eff}}$ ) is applied a simple formula, which is appropriate for the correlations  
 249 involving smoothed data (Bretherton et al., 1999).

250 
$$N_{\text{eff}} = N \frac{(1 - r_1 r_2)}{(1 + r_1 r_2)} \quad (2)$$

251 where  $r_1$  and  $r_2$  are the lag-1 autocorrelation coefficients corresponding to the two time  
 252 series correlated and  $N$  number of the observations.

253 In the next phase, the  $t$ -statistic is used to test the statistical significance of the  
 254 correlation coefficient:

255 
$$t = |r| [(N_{\text{eff}} - 2) / (1 - r^2)]^{1/2} \quad (3)$$

256 In equation (3),  $r$  is the correlation coefficient between the two variables and  $N_{\text{eff}}$  is  
 257 effective number used in the testing procedure.

258 According to von Storch and Zwiers (1999), the null hypothesis  $r = 0$ , is tested by  
 259 comparing the  $t$  value in equation (3) with the critical values of  $t$  distribution with  $n_e - 2$   
 260 degrees of freedom.

261 The correlated time series must have a Gaussian distribution. For this reason in the present  
 262 study we have also applied ~~and the~~ nonparametric Kendall correlation coefficient, which  
 263 measures ~~of~~ correlation of ~~the~~ ranked data. Applying the algorithm described in Press et al.  
 264 (1992), correlation values and corresponding significance p-levels are obtained. A comparison  
 265 between the Pearson and Kendall correlation coefficients is found in Love et al. (2011),  
 266 where the statistical significance between sunspots, geomagnetic activity and global  
 267 temperature, is tested.

268 Among the statistical methods that might be used to test solar or geomagnetic  
 269 activity signal in the climatic variables, in this study we will take into account also ~~on~~ testing  
 270 the statistical significance of the amplitude of the power spectra in time series. Testing the  
 271 statistical significance of the peaks ~~of~~ 1 from an analysis of a time series by power  
 272 spectra ~~is~~ usually ~~by~~ by building a ~~reference~~ spectrum (background) and comparing the  
 273 amplitude ~~of~~ spectrum analyzed time series ~~based~~ spectrum amplitudes. This ~~is~~ a series  
 274 based on ~~noise~~ or most often ~~a~~ red noise ~~series~~ (Ghil et al. 2002, To ~~and~~ and Campo,  
 275 1998). ~~All~~ all amplitudes above the background noise amplitudes are considered  
 276 significant. But to test how significant are these peaks are testing their statistical significance  
 277 compared with different levels of significance ~~desired~~.

278 ~~significance~~ test requires null hypothesis significance ~~for~~ spectra ~~analysis~~, the null  
 279 hypothesis is that the time series has no significant peak and spectral ~~estimation~~ differs from  
 280 the ~~noise~~ spectrum ~~(background)~~. Rejection of the null hypothesis means accepting peaks of  
 281 the spectrum series of observations that exceed a certain level of significance. As shown in  
 282 Mann and Less (1996) theoretical justifications exist for considering red noise as noise  
 283 reference ~~(background)~~ for climate and hydrological time series.

284 The power spectra achieved in this study were estimated by multitaper method (MTM)  
 285 (Thomson, 1982, Ghil et al., 2002, Mann and Less (1996)). The MTM procedure is a  
 286 nonparametric technique that does not require a priori a model for the generation of time  
 287 series analysis, while harmonic spectral analysis assumes that the data generation process  
 288 include components ~~purely~~ ~~periodic~~ and white noise which are overlapped (Ghil et al., 2002).

289 In Mares et al. (2016), more practical details were given on estimating background  
 290 noise and significance of power spectra peaks, for the applications referring to the influence of  
 291 the Palmer drought indices in the Danube discharge.

292

293

294

295 **4 Results and discussions**

296

297 **4.1 Connection between atmospheric circulation at the large scale and climate**  
298 **events at regional or local scale**

299

300 The atmospheric circulation at the large scale is quantified in this paragraph by North  
301 Atlantic Oscillation index (NAOI), Greenland Balkan Oscillation Index (GBOI) and indices  
302 that highlight the blocking type circulation. The direct impact of NAO is less obvious than  
303 GBO impact for the surrounding areas of the lower Danube basin as revealed in this study and  
304 in previous investigations (Mares et al., 2013b, 2014, 2015a,b 2016a,b).

305

306 The high correlations between GBOI and precipitation are stable over time (Table 1).  
307 From how GBO and NAO indices are defined, they have opposite signs. Temporal evolution  
308 for winter of the first principal component (PC1) for the precipitation in the Danube basin in  
comparison with GBOI values is given in Fig.3.

309

310 The details on the stations are given in Fig.4, where are presented the correlation  
311 coefficients between winter precipitation at 15 stations and NAOI and GBOI for two periods  
312 1916-1957 and 1958-1999. From this figure, it is clear that the GBOI signal is stronger than  
313 NAO signal, except for the first stations located in the upper basin of the Danube.

314

315 Since the Danube discharge estimation in spring season with some anticipation has  
316 great importance for the economic sector of Romania, the best predictors at the large scale for  
317 Orsova discharge in spring, with one season anticipation (winter) were revealed, with high  
318 confidence level (> 99%): GBOI as well as the atmospheric circulation of blocking type,  
319 quantified by European blocking index (EBI). The Figure 5 shows spring Orsova discharge  
320 (standardized) in comparison with European blocking index ( $R = -0.54$ ) and GBOI ( $R = 0.53$ )  
321 for winter in the period 1948-2000. The opposite signs of the Orsova discharge correlations  
322 with EBI and GBOI are due to the definitions of the two indices. The negative correlations  
323 between discharge and EBI can be explained as follows. As shown in Davini et al. (2012), the  
324 midlatitude traditional blocking localized over Europe, uniformly present in a band ranging  
325 from the Azores up to Scandinavia, leads to a relatively high pressure field in most of Europe.  
326 This field of high pressure, which defines a positive blocking index, and is not favorable for  
327 precipitation, leads to ~~in~~ low discharge of the Danube at Orsova. A positive correlation  
328 coefficient between the Danube discharge at Orsova and GBOI  means that a positive GBO  
329 index lead to a low pressure in the Danube basin area and therefore high discharge.

330

331 The role of the atmospheric circulation of blocking type on events in the Danube Basin  
332 is described in many papers, including Mares et al. (2006), Blöschl et al. (2013).

333

334 **4.2 Testing predictor variables for estimating the discharge in the Danube lower basin**  
**(1901-2000)**

335

336 To underline the contribution of the nine predictors, defined at the 15 stations in the  
337 Danube basin, described in Section 2, we represented in Figure 6 the correlation coefficients  
338 between Danube discharge at Orsova (lower basin) and these predictors for each of the four  
339 seasons. PC1 in Fig. 6 represents the first principal component of EOFs development of the  
340 respective fields. If we take into account the confidence level at 99%, of correlation  
341 coefficients for 100 values, it should exceed 0.254. There are many predictors that are  
342 statistically significant at this level of confidence, but we take into consideration only those  
343 having the highest correlation coefficients. As can be seen from Figure 6, the greatest  
344 contribution to the Danube discharge in seasons of spring, summer and fall, brings the  
drought index (depending on precipitation and average temperature), with the correlation

345 coefficients (r) of -0.450 - 0.730 for spring and summer and respectively -0.700 for fall. In  
 346 winter season, the highest contribution to the discharge in lower Danube basin, it has  
 347 precipitation field in the upper and middle basin ( $r = 0.500$ ), followed by GBOI ( $r = 0.430$ ).  
 348 Also, it is revealed that for the spring season, where contribution drought index TPPI is  
 349 lower than in summer and autumn season, the GBOI and DTR can be considered good  
 350 predictors with  $r = 0.420$  and respectively -0.417.

351 Regarding consideration of the predictors with some anticipation to the Danube  
 352 discharge, the significant results obtained with an anticipation of a season, are presented in the  
 353 Fig. 7. For spring, the best predictor is clearly drought index (TPPI), taken in winter ( $r =$   
 354 0.62), and also for summer discharge, TPPI in spring is a significant predictor ( $r = -0.55$ ), but  
 355 quite closely related this is the spring precipitation field quantified by PC1 ( $r = -0.53$ ).

356 The results obtained in this study are consistent with those of Mares et al. (2016a),  
 357 where that the Palmer drought indices were found good predictors for the discharge in lower  
 358 basin.

359  
360

### 361 4.3 Solar/geomagnetic signal in the climate fields in Danube basin

362

363 Solar activity was represented by Wolf numbers for the period 1901-2000 and by 10.7-  
 364 cm solar flux for the period 1948-2000. Although the solar flux is closely correlated with  
 365 Wolf numbers, these values are not identical, the correlation coefficient varying with the  
 366 season (0.98-0.99). The geomagnetic activity was quantified by *aa* index for the two periods  
 367 analyzed (1901-2000 and 1948-2000). Regarding the link between solar activity and  
 368 geomagnetic, details are found in Demetrescu and Dobrica (2008).

369 Solar/geomagnetic signal was tested by: correlative analyses (simultaneous and cross  
 370 correlation), composite maps and spectral analyses. Before correlative analysis, data were  
 371 filtered using low and band pass filters for the terrestrial variables and only band pass filters  
 372 for the solar / geomagnetic indices.

373 Related to the low pass filter, the Mann filter (1 2004, 2008) was applied with  
 374 three variants that eliminate frequencies corresponding the periods lower than 8, 10 and 20  
 375 years. The analysis revealed that from the three variants, time series cutoff 8, responded best  
 376 to variations in solar / geomagnetic activities.

377 In many investigations, significant solar signal in the terrestrial variables, have been  
 378 obtained applying band pass filters, for isolating the frequency bands of interest (Lohmann et  
 379 al., 2004, Dima et al, 2005, Prestes et al. 2011, Echer et al. 2012, Wang and Zhao, 2012).

380 In the present study we apply a band pass filter with the three frequency bands: (4-  
 381 8yr), (9-15yr) and (17-28 yr). Because after the filtering process, the time series show a  
 382 strong autocorrelation, to test the statistical significance of the link between the terrestrial and  
 383 solar variables, we use the *t-test*, which takes into account the effective number of  
 384 independent variables and the correlation coefficient between two series. The effective  
 385 number is determined in function of the serial correlations of the two series analyzed. Details  
 386 are given in Section 2. The most significant results were obtained for the filtered terrestrial  
 387 variables, taken with some lags related to solar or geomagnetic activity.

388

#### 389 4.3.1 Simultaneously signal

390

391 The Table 2 presents some of the results that have a confidence level higher or least of  
 392 95%, which worth to be taken into account for the analysis period of 100 years (1901-2000).  
 393 Here are presented only the results simultaneously for three categories of data: non-filtered  
 394 (UF), smoothed by low pass filter (LPF), eliminating, the periods less than or equal to 8 years,

395 only for terrestrial variables, and band pass filter (BPF) applied for both time series (terrestrial  
 396 and solar ~~geomagnetic indices~~ magnetic indices).

397 ~~Since~~ not all variables have a normal distribution, the Kendall's coefficient was  
 398 associated Pearson's coefficient. ~~The nonparametric Kendall coefficient is valid for time~~  
 399 ~~series that do not have a normal distribution.~~ There are cases when the difference between the  
 400 two correlation coefficients is relatively high and this difference may be due to statistical  
 401 distribution that deviates from normal.

402 As can be seen from Table 2, smoothing time series lead to improved correlation  
 403 coefficients, the most significant results were obtained by band-pass filter with frequency  
 404 corresponding to 9-15 yr. Also, tests were achieved and 17-28 yr, but although, highest  
 405 correlation coefficients were obtained, it is difficult to take a decision, because the effective  
 406 number is very small (about 5 years), due to serial correlation very high, caused by such  
 407 filters. For such filtering are necessary much larger sets of data. An example is given in Tab. 2  
 408 to test the correlation between the GBOI and Wolf number during fall season.

409 The results presented in ~~the~~ Table 2, related to the significant correlations indicated by  
 410 Pearson coefficients ( $r$ ), are supported by Kendall correlation coefficients ( $\tau$ ), and their levels  
 411 of significance ( $p$ ). Bold lines means there are at least two situations for the same season  
 412 (filtered or unfiltered data) having a ~~significantly~~ CL.

413 As can be seen from Table 2, highest correlations with aa, were obtained during the  
 414 summer season with  $r = 0.796$  for temperature and with  $r = -0.721$  for precipitation, for a  
 415 smoothing by a BPF with the band (9-15yr). Also, in summer, it is worth ~~to~~ mention the aa  
 416 signal in drought index (TPPI) with ~~the~~ correlation ~~is~~ 0.787, corresponding filtering with (9-  
 417 15 yr). From the definition of this index, it reflects the behavior of both temperature and  
 418 precipitation, but the sign is given by temperature. It can be ~~noting~~ that drought index TPPI,  
 419 which is a combination of temperature and precipitation, responds better to signal aa,  
 420 compared to PC1\_PP. Therefore, a geomagnetic activity maximum (minimum) determines a  
 421 situation of drought (wet) in the Danube basin during spring and summer.

422 Regarding solar activity signal in temperatures and precipitation, the highest  
 423 correlation coefficients were found for the fall season (0.699) and respectively for spring (-  
 424 0.538) in the band filter (9-15 yr). From the Table 2, are observed correlations with the  
 425 number Wolf, with a particularly high confidence level (> 99%) in the case of considering  
 426 time series smoothed by the band (4-8 yr), as atmospheric circulation index GBOI (summer  
 427 and winter).

428 The results obtained in the present investigation, referring to the temperature and  
 429 precipitation variables are in accordance with the ones from Dobrica et al. (2009, 2012),  
 430 where have been analysed the ~~annually~~ mean of long time series (100–150 years) for the  
 431 temperature and precipitation records from 14 meteorological stations in Romania. There are  
 432 some differences, because in this investigation, fields of temperature and precipitation are  
 433 taken on another area, smoothing procedures are different and the analysis is done on each  
 434 season separately. However, the correlations with the geomagnetic aa index and Wolf  
 435 numbers have the same sign, ie positive for temperatures and, negative for precip  
 436 respectively.

437 Reducing the number of effective observations, ~~when is applied a smoothing~~, is  
 438 discussed in Palamara and Bryant (2004), where they test the statistical significance of the  
 439 relationship between geomagnetic activity and the Northern Annular Mode.

440 Although the results obtained here by the BPF shows the largest correlation  
 441 coefficients, however those obtained by BPF (9-15) must be analyzed together with resu  
 442 obtained by other filters. An example is the solar signal, quantified by Wolf number, in the  
 443 drought index (TPPI), for which in the spring, unfiltered data, filtered by the low pass filter,  
 444 and those by BPF (4-8 and 9-15) indicate correlations with confidence level higher than 90%,

445 it means that significance of the correlation in this case, does not depend on the time series  
 446 size.

447 Taking into account both signals of the geomagnetic and solar activity, we can notice  
 448 that during spring, TPPI has the best respond for unfiltered or filtered time series.

449 Considering the importance of the Danube discharge in our study, we analyze solar /  
 450 geomagnetic signals in this variable. Thus, the *aa* signal in Danube discharge at Orsova  
 451 (Q\_ORS), is seen as the most significant, during the summer season with correlation  
 452 coefficient  $r = -0.656$ . But considering our criteria above enumerated, ie significant  
 453 correlations in at least two cases, it is clear that we must focus on the discharge behavior in  
 454 fall (Table 2), for which the smoothing by LPF and BPF (9-15) lead to the significant  
 455 response to *aa* impulse.

456 In the following, we present results obtained by analyzing the terrestrial and solar  
 457 geomagnetic data for the period 1948-2000. Although the time series are relatively short, was  
 458 considered this period because some of the atmospheric variables, as indices that define the  
 459 type blockage 500 hPa, are available only in 1948. Also 10.7 cm solar flux that defines more  
 460 clearly solar activity is just beginning in this period. In addition, we wanted to see if it  
 461 improves the relationship between the terrestrial and solar indices, taking separately the years  
 462 with positive or negative phase of Quasi-Biennial Oscillation (QBO).

463 In the Table 3 are presented the correlation coefficients with a high confidence level  
 464 ( $>95\%$ ), obtained from the simultaneous correlative analyzes between terrestrial variables and  
 465 geomagnetic (*aa*), and solar activity (flux 10.7cm) indices on the other hand. It is observed that  
 466 due to short time series, the smoothing by the band pass filter (9-15), although leads to the  
 467 correlation coefficients with high confidence level, the number of degrees of freedom is quite  
 468 small.

469 For this period of 53 years (1948-2000), the smoothing by BPF with the band (4-8 yr)  
 470 appears most appropriate, especially for highlighting solar signal, where all three blocking  
 471 indices considered in this paper, respond significantly to the solar impulse.

472 The solar or geomagnetic signals in the terrestrial variables can be emphasized also by  
 473 the periodicities estimation by means of the power spectra. In the present study the power  
 474 spectra were estimated by means of multitaper method (MTM). For the time series of  
 475 unfiltered European blocking index (EBI) during winter, the power spectra given in the Fig.8a  
 476 reveals that the most significant periodicity is related to QBO (2.4 years), and with an  
 477 approximately 90% confidence level are the peaks at 10.7 and 14.2 years, which may be  
 478 linked to 11-year solar/geomagnetic cycle. In Fig. 8b, which represents the power spectrum  
 479 for EBI in the spring, the only significant peak with a confidence level of 95% is situated at  
 480 10 years. This is consistent with the results shown in Table 3, where during spring, the time  
 481 series of blocking index EBI, both unfiltered and filtered by the band pass filter (4-8) have  
 482 significant correlations with the *aa* geomagnetic index. Also, in winter (Fig. 8a), the EBI's  
 483 response to solar activity, quantified by the Wolf number, is statistical significant with CL  
 484 almost 99%. If we take only spring season, the best significant peak related to QBO (Fig. 8c)  
 485 is found in blocking index over Atlantic European region (AEBI).

486 Graphical representation of unfiltered time series was given to see whether the there  
 487 are solar/ geomagnetic signals in the original series. The power spectra of the filtered series  
 488 were not shown, because these series show peaks corresponding to the frequencies remaining  
 489 after filtering procedure.

490 Regarding the period of 53 years (1948-2000), significant signals of the solar activity  
 491 quantified by solar flux 10.7cm were obtained for spring and summer in the Danube discharge  
 492 at Orsova (Q\_ORS), with different lags, especially to a delay of two years, where both  
 493 unfiltered and filtered time series, indicate statistically significant correlations.

494 Like in the GBOI case, the discharge is inversely, but well correlated with solar  
 495 activity. In Fig. 10a, correlation coefficients are shown at the lags 1-5 for three series,  
 496 unfiltered (UF), smoothed by low pass filter (LPF) and the band pass filter (9-15). It can be  
 497 observed that, if for the unfiltered data, the signal is significant at the lag 1 and 2, for the data  
 498 smoothed by BPF, this signal is at the lags 2, 3 and 4. Taking into account the LPF result,  
 499 can be considered the significant result at the lag 2 years. In the Fig. 10b have been  
 500 shown the coherent time solutions of the solar flux and discharge, smoothed by BPF (9-15)  
 501 with a lag of three years, where, the correlation coefficient is highest (-0.769) and CL is 99%  
 502 From the above results, we can highlight that the Danube discharge in the lower basin,  
 503 at the 2 or 3 years during spring and summer, after a maximum (minimum) solar, will be  
 504 lower (higher).

505 A different response to solar activity was found in the time series of the index that  
 506 defines a atmospheric circulation of blocking type over Atlantico-European region, for the  
 507 period 1948-2000, during the winter season. As can be seen in Fig. 11, the response this index  
 508 to the solar activity is significant with a delay of two years and three years compared to the  
 509 solar flux. It is worth noting that in this case, the filtering process does not lead to an  
 510 improvement of the significance of the correlation, even if its value increases. Thus it is  
 511 necessary a rigorous test for correlation's significance, especially for data smoothed.  
 512 Therefore, we might conclude that about 2-3 years after producing a maximum (minimum)  
 513 solar, winter, atmospheric circulation of blocking type is enhanced (weakened) over the  
 514 Atlantico-European region.

### 515 516 517 4.3.3 QBO role

518 Regarding QBO influence on the relationship between solar activity and terrestrial  
 519 parameters, there are several investigations (Van Loon and Labitzke, 1988; Bochníček et  
 520 al. 1999, Huth et al., 2009), which demonstrated that QBO phase is very important for  
 521 emphasizing these links. We see in QBO mainly an important modulator of the impact of  
 522 solar activity on the phenomena of the lower troposphere. To test these findings, in this paper  
 523 the years with east QBO phase, during winter months have been selected, and were made  
 524 correlations between solar flux and more terrestrial variables. Winter, from the atmospheric  
 525 indices of blocking type at 500 hPa, best response at the QBO signal, was found in the  
 526 blocking over the European sector (EBI), with power spectrum shown in Fig. 8a. But the  
 527 correlation coefficient between the solar flux and the unfiltered EBI during winter, for all  
 528 those 53 years, is 0.15 and not is statistically significant. By selecting only the years with  
 529 QBO in the east phase in the winter months (34 cases), the correlation coefficient is 0.32 at  
 530 the confidence level around 95%. It is interesting that although the power spectrum (Fig. 8a)  
 531 highlights significant peaks related to the QBO (2.4 and 2.7 ani), the correlation coefficient  
 532 between EBI and QBO is insignificant. This suggests that the spectral representation is very  
 533 useful in time series analysis and the QBO phases modulate the connection between solar  
 534 activity and blocking circulation.

535 It is enlightening solar impact (by flux) on atmospheric circulation in the lower troposphere,  
 536 during the east phase of QBO, when the solar maximum is associated with blocking event over the  
 537 Northern Atlantic and north-western Europe (Fig. 12a), and a geopotential with a opposite  
 538 distribution that occurs during the solar minimum. (Fig. 12b).

539 The advantage of the composite maps, used to outline the response to the solar signal, is  
 540 shown in Sfica et al. (2015), which specifies that through these composite maps, nonlinearities are  
 541 taken into account, compared to using linear methods.

543 Our findings, presented in the Fig. 12, are in concordance with Barriopedro et al. (2008),  
 544 namely, QBO is a modulator of the atmospheric circulation transformation from a blocking  
 545 type circulation to a zonal one and vice versa, under the solar impact.

546 We mention that in the period 1948-2000 were recorded 34 months of winter (DJF) in which  
 547 occurred east QBO phase and the solar flux has produced in the lower troposphere an atmospheric  
 548 blocking events, or a zonal atmospheric circulation, at middle and higher latitudes, depending on the  
 549 state of maximum or minimum solar activity, respectively.

550

551

## 552 5 Conclusions

553

554 In the present investigation, we focused on finding predictors for the discharge in the  
 555 Danube lower basin, which present a high level of statistical significance.

556 In the first part of the paper we tested the predictors for the discharge, from the field  
 557 of temperature, precipitation, cloud cover in the Danube basin, and indices of atmospheric  
 558 circulation over the European Atlantic region. For climate variables defined in the Danube  
 559 basin, as predictor we used only the first principal component (PC1) of the EOFs  
 560 decomposition and a drought index (TPPI) derived from the standardized temperature and  
 561 precipitation.

562 The atmospheric circulation has been quantified by Greenland Balkan Oscillation  
 563 (GBO) and North Atlantic Oscillation (NAO) indices and the blocking type indices. The  
 564 analysis was performed separately for each season and on the two period (1901-2000) and  
 565 (1948-2000).

566

Main statistically significant results for this part of our research are the following:

567

1. The correlative analyzes simultaneously for each season, revealed that, except for the winter season, drought index (TPPI) has the highest weight to the discharge variability in the lower basin of the Danube.
2. Testing the predictors, in order to see their predictive capacity, with a lag of several months in advance of discharge, concluded that TPPI in winter and spring is a good indicator for the Danube discharge in spring and summer respectively.
3. We demonstrated that for the winter, GBOI has an influence on the climate variables in the Danube middle and lower basin more significant than NAOI.
4. Analysis for the period 1948-2000, reveals that in winter, the GBOI weight for the Danube discharge is similar to those of the blocking index over the European sector.

578

In the second part of the paper, we focused on solar/geomagnetic signals in the terrestrial variables. Because the solar and geomagnetic variables as well as the smoothing procedures through various filters, respectively low pass filter and band pass filters applied in this investigation, shows strong serial correlations, all correlative analyzes were performed through rigorous testing of statistical significance. The number of observations was reduced to the effective number of degrees of freedom, corresponding to the independent observations.

584

The filtering procedures led to improvement of the correlative analyses between solar or geomagnetic activity and terrestrial variables, under the condition of a rigorous test of the statistical significance.

587

The main findings of our research for this topic are the following:

588

5. The most significant signals of solar/geomagnetic activities were obtained in the drought indicator (TPPI). Because the precipitation does not respond just as well as, temperatures to the solar signal, is preferred analysis TPPI variable in stead of temperatures and precipitation separately.
6. From the analysis of correlations with the lags from 0 to five years delay of the terrestrial variables in comparison with the solar/geomagnetic activity, we obtained



594 very different results, depending on the season and on the considered variables, as well  
 595 as on the filtering procedure. Such, we might conclude that in winter, about 2-3 years  
 596 after producing a maximum (minimum) solar, winter, atmospheric circulation of  
 597 blocking type is enhanced (weakened) over the Atlantic-European region. Also, it was  
 598 found that the Danube discharge in the lower basin, at the 2 or 3 years during spring  
 599 and summer, after a maximum (minimum) solar, will be lower (higher).

600 7. A terrestrial variable that respond to the solar signal, even more significant than to the  
 601 geomagnetic signal, is atmospheric circulation index GBO, in summer. Therefore, at  
 602 the 2-3 years after a maximum (minimum) of solar activity, expects a response of  
 603 atmospheric circulation in the Atlantic-European region, quantified by GBOI, by a  
 604 diminution of this index, i.e. decrease (increase) of pressure in Greenland area and an  
 605 increase (decrease) in atmospheric pressure in the Balkans.

606 8. By multitaper method (MTM) procedure, the power spectra have highlighted both  
 607 quasi-periodicities related to solar activity and the other oscillations such as QBO. In  
 608 the time series of AEBI (spring), and EBI (winter) the most significant periodicity is  
 609 related to QBO (2.2-2.7 years) and with an approximately 90% confidence level there  
 610 are peaks at 10-14 years, which may be linked to 11-year solar cycle.

611 9. The composite maps revealed that solar impact (by flux) on atmospheric circulation in  
 612 the middle troposphere, during the east phase of QBO, is associated with blocking  
 613 event over the Northern Atlantic and north-western Europe, and a geopotential with a  
 614 opposite distribution that occurs during the solar minimum.

615 In this study, we focused only on observational data, so that in next our investigations, we will  
 616 take into account significant predictors for the Danube basin found in this investigation, like  
 617 GBOI, TPPI and atmospheric blocking indices from the outputs of the simulation  
 618 models. Also we will take into account non-stationarities and non-linearities associated with  
 619 the major modes of climate variability.

620  
 621 *Acknowledgements.* This study has been achieved under VALUE: COST Action ES1102.

## 623 References

625 Barriopedro, D., García-Herrera, R., and Huth, R.: Solar modulation of Northern Hemisphere  
 626 winter blocking, *J. Geophys. Res.*, 113, D14118, doi:10.1029/2008JD009789, 2008.

627 Benestad, R.E.: Schmidt GA: Solar trends and global warming, *J. Geophys. Res.* 114:D14101,  
 628 doi:10.1029/2008JD011639, 2009.

629 Blöschl, G., Nester, T., Komma, J., Parajka, J., and Perdigão, R. A. P.: The June 2013 flood in  
 630 the Upper Danube Basin, and comparisons with the 2002, 1954 and 1899 floods, *Hydrol.*  
 631 *Earth Syst. Sci.*, 17, 5197–5212, doi:10.5194/hess-17-5197-2013, 2013.

632 Bochníček, J., Hejda, P., and Pýcha, J.: The effect of geomagnetic and solar activity on the  
 633 distribution of controlling pressure formations in the Northern Hemisphere in winter,  
 634 *Studia geophysica et geodaetica*, 43(4), 390-398, 1999.

635 Bretherton, C.S., Widmann, M., Dymnikov, V.P., Wallace, J.M. and Bladé, I.: The effective  
 636 number of spatial degrees of freedom of a time-varying field, *Journal of climate*, 12(7),  
 637 1990-2009, 1999.

638 Brugnara, Y., Brönnimann, S., Luterbacher, J., and Rozanov, E.: Influence of the sunspot  
 639 cycle on the Northern Hemisphere wintertime circulation from long upper-air data sets,  
 640 *Atmos. Chem. Phys.*, 13, 6275-6288, doi:10.5194/acp-13-6275-2013, 2013.

641 Cubasch, U., Voss, R., Hegerl, G.C., Waszkewitz, J. and Crowley, T.J.: Simulation of the  
 642 influence of solar radiation variations on the global climate with an ocean-atmosphere  
 643 general circulation model, *Climate Dynamics*, 13(11), 757-767, 1997.

644 Davini, P., Cagnazzo, C. Gualdi, S. and Navarra, A.: Bidimensional Diagnostics, Variability,  
 645 and Trends of Northern Hemisphere Blocking, *J. Climate*, 25, 6496–6509, 2012.

646 Demetrescu, C. and Dobrica,V.: Signature of Hale and Gleissberg solar cycles in the  
 647 geomagnetic activity, *J. Geophys. Res.*, 113, A02103, doi:10.1029/2007JA012570, 2008.

648 Dima, M., Lohmann, G. and Dima I.: Solar-Induced And Internal Climate Variability at  
 649 decadal time scales, *Int. J. Climatol.*, 25: 713–733, 2005.

650 Dobrica, V., C. Demetrescu, Boroneant, C. and Maris G.: Solar and geomagnetic activity  
 651 effects on climate at regional and global scales: Case study—Romania, *J.Atmos. Sol.-Terr.*  
 652 *Phy.*, 71 (17-18), 1727-1735, doi:10.1016/j.jastp.2008.03.022, 2009.

653 Dobrica V., Demetrescu, C.: On the evolution of precipitation in Central and South-Eastern  
 654 Europe and its relationship with Lower Danube discharge, in: AGU Fall Meeting  
 655 Abstracts, 11, 1030, 2012.

656 Drobyshev, I., Niklasson, M., Linderholm, H.W., Seftigen, K., Hickler, T., Eggertsson, O.:  
 657 Reconstruction of a regional drought index in southern Sweden since AD 1750, *The*  
 658 *Holocene* 21(4) 667-679, doi: 10.1177/0959683610391312, 2011.

659 Ebisuzaki, W.: A Method to Estimate the Statistical Significance of a Correlation when the  
 660 Data is Serially Correlated, *J. Climate*, 10:2147–2153, 1997.

661 Echer, M. S., Echer, E., Nordemann, D. J. R., and Rigozo, N. R.: Multi-resolution analysis of  
 662 global surface air temperature and solar activity relationship, *Journal of Atmospheric and*  
 663 *Solar-Terrestrial Physics*, 71(1), 41-44, 2009.

664 Echer, M.S., Echer, E., Rigozo, N.R., Brum, C.G.M., Nordemann, D.J.R., and Gonzalez,  
 665 W.D.: On the relationship between global, hemispheric and latitudinal averaged air surface  
 666 temperature (GISS time series) and solar activity, *Journal of Atmospheric and Solar-*  
 667 *Terrestrial Physics*, 74, pp.87-9,2012.

668 El-Janyani, S., Massei, N., Dupont, J.P., Fournier, M. and Dörfliger, N.: Hydrological  
 669 responses of the chalk aquifer to the regional climatic signal, *Journal of Hydrology*, 464,  
 670 485-493, 2012.

671 Ghil, M., Allen, M.R., Dettinger, M.D., Ide, K., Kondrashov, D., Mann, M.E., Robertson,  
 672 A.W., Saunders, A., Tian, Y., Varadi, F., Yiou, P.: Advanced spectral methods for  
 673 climatic time series, *Reviews of Geophysics* 40 (1), doi: 10.1029/2001RG000092, 2002.

674 Gray, L. J., A. A. Scaife, D. M. Mitchell, S. Osprey, S. Ineson, S. Hardiman, N. Butchart, J.  
 675 Knight, R. Sutton, and Kodera K.: A lagged response to the 11 year solar cycle in observed  
 676 winter Atlantic/Euro pean weather patterns, *J. Geophys. Res. Atmos.*, 118, 13, 405–13,  
 677 420, doi:10.1002/2013JD020062, 2013.

678 Hertig, E., Beck,C., Wanner,H., Jacobbeit, J.: A review of non-stationarities in climate  
 679 variability of the last century with focus on the North Atlantic-European sector, *Earth-*  
 680 *Science Reviews* 147, 1–17, doi:[10.1016/j.earscirev.2015.04.009](https://doi.org/10.1016/j.earscirev.2015.04.009), 2015.

681 Hurrell, JW, Kushnir Y, Visbeck M, Ottersen G: Research Abstracts EGU2007-A-08910  
 682 9:1029- 2003. An overview of the North Atlantic Oscillation. In: Hurrell, J.W., Kushnir,  
 683 Y., Ottersen, G., Visbeck, M. (Eds.), *The North Atlantic Oscillation, Climatic Significance*  
 684 *and Environmental Impact*, AGU *Geophysical Monograph*, 134, 1–35, 2003.

685 Huth, R., Pokorná, L., Bochníček, J., and Hejda, P.: Combined solar and QBO effects on the  
 686 modes of low-frequency atmospheric variability in the Northern Hemisphere, *Journal of*  
 687 *Atmospheric and Solar-Terrestrial Physics*, 71(13), 1471-1483, 2009.

688 Lejenas, H., and Okland, H.: Characteristics of Northern Hemisphere blocking as determined  
 689 from a long time series of observational data, *Tellus* , 35A, 350-362, 1983.

690 Lohmann, G., Rimbu, N., and Dima, M.: Climate signature of solar irradiance variations:  
 691 analysis of long-term instrumental, historical, and proxy data, *International Journal of*  
 692 *Climatology*, 24(8), pp.1045-1056, 2004.

693 Love, J. J., K. Mursula, V. C. Tsai, and Perkins, D. M.: Are secular correlations between  
 694 sunspots, geomagnetic activity, and global temperature significant?, *Geophys. Res. Lett.*,  
 695 38, L21703, doi: 10.1029/2011GL049380, 2011.

696 Mann, M. E. and Lees, J.: Robust estimation of background noise and signal detection in  
 697 climatic time series, *Climatic Change*, 33, 409–445, 1996.

698 Mann, M. E.: On smoothing potentially non-stationary climate time series, *Geophys. Res.  
 699 Lett.*, 31, L07214, doi: 10.1029/2004GL019569, 2004.

700 Mann, M. E.: Smoothing of climate time series revisited, *Geophys. Res. Lett.*, 35, L16708,  
 701 doi: 10.1029/2008GL034716, 2008.

702 Mares, I., Mares, C., Mihailescu, M.: NAO impact on the summer moisture variability across  
 703 Europe, *Physics and chemistry of the Earth*, 27, 1013-1017, 2002.

704 Mares C., Mares, I., and Stanciu, A: On the possible causes of the severe drought in the  
 705 Danube lower basin in 2003, in: Proceedings of the International Conference on "Water  
 706 Observation and Information System for Decision Support" Ohrid, Republic of  
 707 Macedonia, 23- 26 May., 2006.  
 708 [http://balwois.mpl.ird.fr/balwois/administration/full\\_paper/ffp-672.pdf](http://balwois.mpl.ird.fr/balwois/administration/full_paper/ffp-672.pdf) )

709 Mares, C., Mares, I. and Stanciu, A.: Extreme value analysis in the Danube lower basin  
 710 discharge time series in the 20<sup>th</sup> century, *Theoretical and Applied Climatology*, 95, 223-  
 711 233, 2009.

712 Mares, I., Mares,C., Stanciu,A., and Mihailescu, M.: On the climate models performances to  
 713 simulate the main predictors that influence the discharges in the Danube middle and lower  
 714 basin, *Geophysical Research Abstracts*, 13, EGU2011-2325, EGU General Assembly,  
 715 2011.

716 Mares, C., Mares,I. Stanciu, A., and Mihailescu,M.: North Atlantic Oscillation (NAO)  
 717 influence on the Danube lower basin, *Proc. Fifth Int. Scientific Conf. on Water, Climate  
 718 and Environment: BALWOIS 2012*, Ohrid, Macedonia, Balwois, 2012-771, 2012.

719 Mares, I., Mareş, C. and Mihăilescu M.: On the statistical significance of the sea level  
 720 pressure climatic signal simulated by general circulation models for the 21 st century over  
 721 Europe. *Rev. Roum. Géophysique*, 25–40, 2013a.

722 Mares, I., Mareş, C., and Mihailescu, M.: Stochastic modeling of the connection between sea  
 723 level pressure and discharge in the Danube lower basin by means of Hidden Markov  
 724 Model, *EGU General Assembly Conference Abstracts*, 15, 7606, 2013b.

725 Mares, I., Dobrica, V., Demetrescu, C. and Mares,C.: Moisture variability in the Danube  
 726 lower basin: an analysis based on the Palmer drought indices and the solar/geomagnetic  
 727 activity influence, *Geophysical Research Abstracts*, 16, EGU2014-6390, 2014.

728 Mares, C., Adler M. J., Mares I, Chelcea, S., Branescu, E.: Discharge variability in  
 729 Romania using Palmer indices and a simple atmospheric index of large-scale circulation,  
 730 *Hydrological Sciences Journal*, doi: 10.1080/02626667.2015.1006233), 2015a.

731 Mares, I., Dobrica,V., Demetrescu, C., and Mares, C.: Influence of the atmospheric blocking  
 732 on the hydrometeorological variables from the Danube basin and possible response to the  
 733 solar/geomagnetic activity, *Geophysical Research Abstracts*, 17, EGU2015-4154-3,2015,  
 734 EGU General Assembly 2015 (PICO2.6), 2015b.

735 Mares, C., Mares,I., and Mihailescu, M.: Identification of extreme events using drought  
 736 indices and their impact on the Danube lower basin discharge, *Hydrological Processes*,  
 737 doi: 10.1002/hyp.10895), 2016a.

738 Mares, I., Dobrica, V. Demetrescu, C.,and Mares, C.,: Hydrological response in the Danube  
 739 lower basin to some internal and external forcing factors of the climate system,  
 740 *Geophysical Research Abstracts*, 18, EGU2016-7474, EGU General Assembly 2016b.

741

742 Massei, N., Laignel, B., Deloffre, J., Mesquita, J., Motelay, A., Lafite, R., and Durand, A.:  
 743 Long-term hydrological changes of the Seine River flow (France) and their relation to the  
 744 North Atlantic Oscillation over the period 1950–2008, International journal of  
 745 Climatology, 30(14), pp.2146-2154, 2010.

746 Palamara, D.R. and Bryant, E.A.: March. Geomagnetic activity forcing of the Northern  
 747 Annular Mode via the stratosphere, in: Annales Geophysicae, 22, No. 3, 725-731, 2004

748 Papadimitriou, L. V., Koutroulis, A. G., Grillakis, M. G., and Tsanis, I. K.: High-end climate  
 749 change impact on European runoff and low flows – exploring the effects of forcing biases,  
 750 Hydrol. Earth Syst. Sci., 20, 1785-1808, doi:10.5194/hess-20-1785-2016, 2016.

751 Press, W. H., S. A. Teukolsky, W. T. Vetterling, and Flannery, B. P.: Numerical Recipes,  
 752 Cambridge Univ. Press, Cambridge, U. K., 1992

753 Prestes, A., Rigozo, N. R., Nordemann, D. J. R., Wrasse, C. M., Echer, M. S., Echer, E., ...  
 754 and Rampelotto, P. H.: Sun–earth relationship inferred by tree growth rings in conifers  
 755 from Severiano De Almeida, Southern Brazil, Journal of Atmospheric and Solar-  
 756 Terrestrial Physics, 73(11), 1587-1593, 2011.

757 Rimbu N, Boroneanț C, Buță C, and Dima M.: Decadal variability of the Danube river flow  
 758 in the lower basin and its relation with the North Atlantic Oscillation, International Journal  
 759 of Climatology., 22(10):1169-79, 2002.

760 Rimbu, N., and Lohmann, G.: Winter and summer blocking variability in the North Atlantic  
 761 region—evidence from long-term observational and proxy data from southwestern  
 762 Greenland, Climate of the Past, 7(2), 543-555, 2011.

763 Rimbu, N., Dima, M., Lohmann, G. and Musat, I.: Seasonal prediction of Danube flow  
 764 variability based on stable teleconnection with sea surface temperature, Geophysical  
 765 Research Letters, 32(21), 2005.

766 Scaife, A. A., Ineson, S., Knight, J. R., Gray, L.J., Kodera, K., and Smith, D. M.: A  
 767 mechanism for lagged North Atlantic climate response to solar variability, Geophys. Res.  
 768 Letts., 40, 434–439, doi:10.1002/grl.50099, 2013.

769 Sfică, L., Voiculescu, M., and Huth, R.: The influence of solar activity on action centres of  
 770 atmospheric circulation in North Atlantic, Ann. Geophys., 33, 207-215,  
 771 doi:10.5194/angeo-33-207-2015, 2015.

772 Thiebaut, H. J., and Zwiers, F. W.: The interpretation and estimation of effective sample size,  
 773 J. Climate Appl. Meteor., 23, 800–811, 1984.

774 Thomson, D. J.: Spectrum estimation and harmonic analysis, IEEE Proc., 70, 1055-1096,  
 775 1982.

776 Torrence, C., and Compo, G. P.: A practical guide to wavelet analysis. Bull. Amer. Meteor.  
 777 Soc., 79, 61–78, 1998.

778 Trenberth, K. E., and Paolino, D. A.: The Northern Hemisphere sea level pressure data set:  
 779 Trends, errors, and discontinuities, Mon. Weather Rev. 108: 855-872, 1980.

780 Turki, I., Laignel, B., Massei, N., Nouaceur, Z., Benhamiche, N., and Madani, K.:  
 781 Hydrological variability of the Soummam watershed (Northeastern Algeria) and the  
 782 possible links to climate fluctuations, Arabian Journal of Geosciences, 9(6), 1-12, 2016.

783 Valty, P., De Viron, O., Panet, I., and Collilieux, X.: Impact of the North Atlantic Oscillation  
 784 on Southern Europe Water Distribution: Insights from Geodetic Data. Earth  
 785 Interactions, 19(10), 1-16, 2015.

786 Van Loon H. and Labitzke, K: Association between the 11-Year Solar Cycle, the QBO, and  
 787 the Atmosphere. Part II: Surface and 700 mb in the Northern Hemisphere in Winter, J.  
 788 Climate, 1, 905–920, 1988.

789 Van Loon, H., and Meehl, G. A.: Interactions between externally forced climate signals from  
 790 sunspot peaks and the internally generated Pacific Decadal and North Atlantic Oscillations,  
 791 Geophys. Res. Lett., 41, 161–166, doi:10.1002/ 2013GL058670, 2014.

792 Von Storch H.V. and Zwiers F. W.: Statistical Analysis in Climate Research. Cambridge  
 793 University Press, 484, 1999.  
 794 Wang, J. S., and Zhao, L.: Statistical tests for a correlation between decadal variation in June  
 795 precipitation in China and sunspot number, J. Geophys. Res., 117, D23117,  
 796 doi:10.1029/2012JD018074, 2012.  
 797 Zanchettin, D., Rubino, A., Traverso, P., and Tomasino, M. : Impact of variations in solar  
 798 activity on hydrological decadal patterns in northern Italy, J. Geophys. Res., 113, D12102,  
 799 doi: 10.1029/2007JD009157, 2008.  
 800 Zwiers, F. W., and von Storch H: Taking Serial Correlation into Account in Tests of the  
 801 Mean. J. Climate, 8, 336\_351, 1995  
 802  
 803

804 Table 1. Correlation coefficient between first principal component (PC1)  
 805 for the precipitation and atmospheric indices NAO and GBO, during winter  
 806

Period	NAOI	GBOI
1916-1957	-0.36	<b>0.75</b>
1958-1999	<b>-0.43</b>	<b>0.84</b>

807  
 808  
 809  
 810 Table 2. Simultaneous correlation (1901-2000) with confidence level (CL) at least 95%, for unfiltered  
 811 (UF) data, terrestrial variables filtered by low pass filter (LPF) and both time series correlated,  
 812 smoothed by band pass filtered and the band is specified in the brackets.  $r$ - Pearson correlation  
 813 coefficient,  $t$ - the values of test  $t$ ,  $\tau$  - Kendall correlation coefficient,  $p$  - significance p-level,  $N_{eff}$  is  
 814 the effective number.  
 815

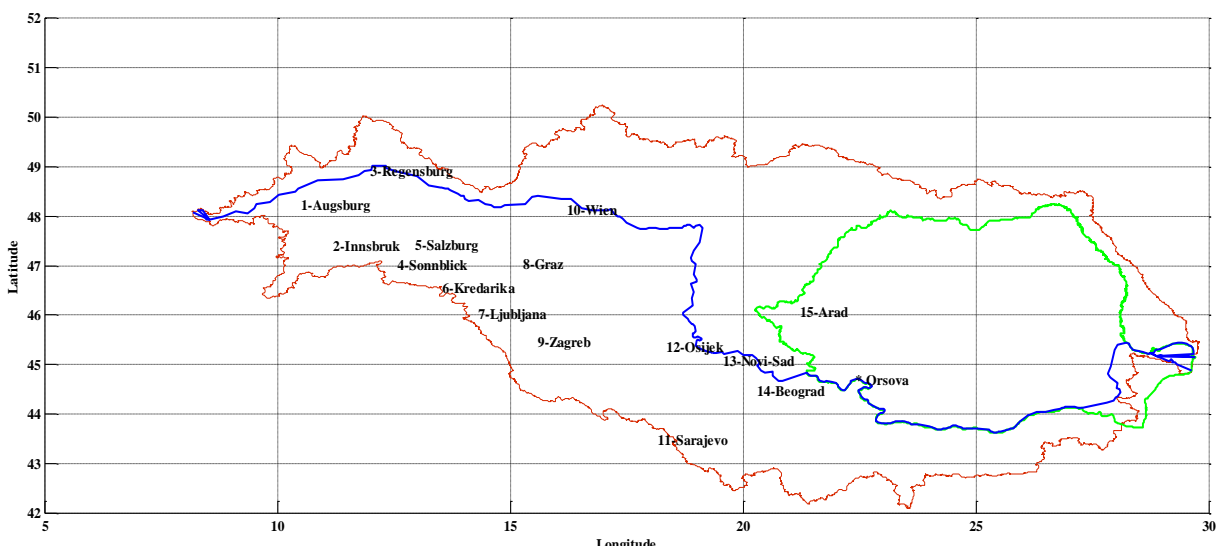
Variable	Season	$r$	$t$	$\tau$	$p$	$N_{eff}$	CL
<i>Correlation with aa</i>							
PC1_TT(UF)	Spring	<b>0.224</b>	<b>2.184</b>	<b>0.137</b>	<b>0.043</b>	<b>92</b>	<b>95%</b>
PC1_TT(4-8)	Spring	<b>0.606</b>	<b>6.457</b>	<b>0.401</b>	<b>0.000</b>	<b>74</b>	<b>99.5%</b>
PC1_TT(UF)	Summer	<b>0.310</b>	<b>2.663</b>	<b>0.206</b>	<b>0.002</b>	<b>69</b>	<b>99%</b>
PC1_TT(LPF)	Summer	<b>0.345</b>	<b>2.037</b>	<b>0.210</b>	<b>0.002</b>	<b>33</b>	<b>95%</b>
PC1_TT(9-15)	Summer	<b>0.796</b>	<b>5.130</b>	<b>0.570</b>	<b>0.000</b>	<b>17</b>	<b>99.5%</b>
PC1_TT(LPF)	Fall	0.453	2.865	0.304	0.000	34	99%
PC1_PP(LPF)	Spring	<b>-0.371</b>	<b>2.201</b>	<b>-0.315</b>	<b>0.000</b>	<b>32</b>	<b>95%</b>
PC1_PP(9-15)	Spring	<b>-0.669</b>	<b>3.437</b>	<b>-0.501</b>	<b>0.000</b>	<b>17</b>	<b>99.5%</b>
PC1_PP(9-15)	Summer	-0.721	3.910	-0.523	0.000	16	99.5%
TPPI(LPF)	Fall	0.452	2.869	0.310	0.000	34	99%
TPPI(UF)	Spring	<b>0.275</b>	<b>2.676</b>	<b>0.186</b>	<b>0.006</b>	<b>90</b>	<b>99%</b>
TPPI(LPF)	Spring	<b>0.299</b>	<b>1.736</b>	<b>0.261</b>	<b>0.000</b>	<b>33</b>	<b>90%</b>
TPPI(4-8)	Spring	<b>0.525</b>	<b>5.313</b>	<b>0.338</b>	<b>0.000</b>	<b>76</b>	<b>99.5%</b>
TPPI(9-15)	Spring	<b>0.402</b>	<b>1.660</b>	<b>0.325</b>	<b>0.000</b>	<b>16</b>	<b>85-90%</b>
TPPI(UF)	Summer	<b>0.224</b>	<b>2.121</b>	<b>0.153</b>	<b>0.025</b>	<b>87</b>	<b>95%</b>
TPPI(LPF)	Summer	0.318	1.921	0.187	0.006	35	~95%
TPPI(9-15)	Summer	<b>0.787</b>	<b>4.856</b>	<b>0.572</b>	<b>0.000</b>	<b>16</b>	<b>99.5%</b>
Q_ORS(LPF)	Fall	<b>-0.324</b>	<b>1.946</b>	<b>-0.210</b>	<b>0.002</b>	<b>34</b>	<b>~95%</b>
Q_ORS(9-15)	Fall	<b>-0.562</b>	<b>2.454</b>	<b>-0.419</b>	<b>0.000</b>	<b>15</b>	<b>95-98%</b>
Q_ORS(9-15)	Summer	-0.656	3.210	-0.470	0.000	16	99%

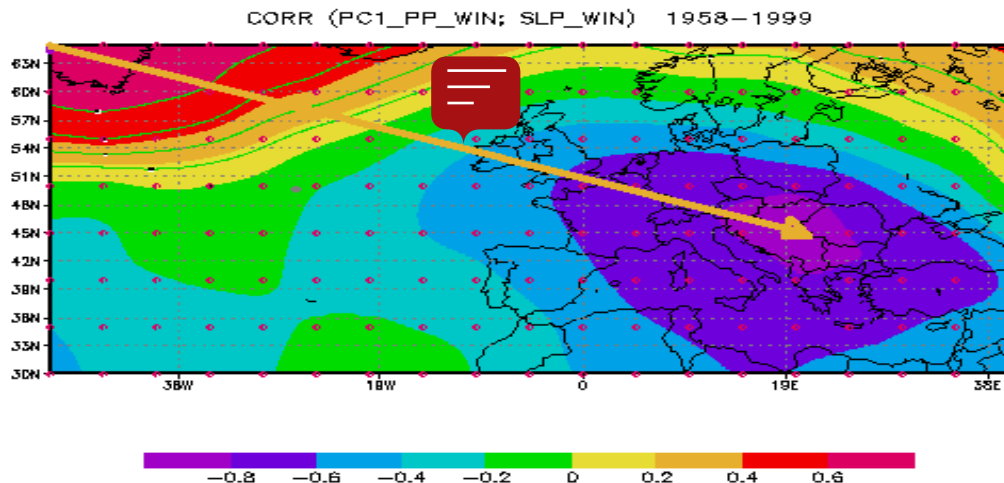
Correlation with Wolf number							
PC1_TT(4-8)	Summer	0.288	2.453	0.157	0.021	68	98%
PC1_TT(9-15)	Fall	0.699	3.770	0.550	0.000	17	99.5%
<b>PC1_PP(4-8)</b>	<b>Spring</b>	<b>-0.242</b>	<b>2.133</b>	<b>-0.190</b>	<b>0.005</b>	<b>75</b>	<b>95-98%</b>
<b>PC1_PP(9-15)</b>	<b>Spring</b>	<b>-0.538</b>	<b>2.417</b>	<b>-0.363</b>	<b>0.000</b>	<b>16</b>	<b>95-98%</b>
PC1_PP(4-8)	Winter	-0.370	3.298	-0.265	0.000	70	>99%
<b>TPPI(UF)</b>	<b>Spring</b>	<b>0.211</b>	<b>1.973</b>	<b>0.148</b>	<b>0.029</b>	<b>85</b>	<b>95%</b>
TPPI(LPF)	Spring	0.299	1.736	0.261	0.000	33	90%
<b>TPPI(4-8)</b>	<b>Spring</b>	<b>0.245</b>	<b>2.154</b>	<b>0.159</b>	<b>0.019</b>	<b>74</b>	<b>95-98%</b>
<b>TPPI(9-15)</b>	<b>Spring</b>	<b>0.585</b>	<b>2.708</b>	<b>0.395</b>	<b>0.000</b>	<b>16</b>	<b>98%</b>
TPPI(9-15)	Fall	0.673	3.796	0.553	0.000	19	99%
GBOI (4-8)	Summer	-0.346	2.982	-0.230	0.001	67	99.5%
GBOI (4-8)	Winter	-0.343	3.169	-0.218	0.001	77	>99%
GBOI (17-28)	Fall	-0.899	3.485	-0.707	0.000	5	95-98%
Q_ORS (4-8)	Winter	-0.263	2.329	-0.163	0.016	75	98%

816  
817  
818  
819

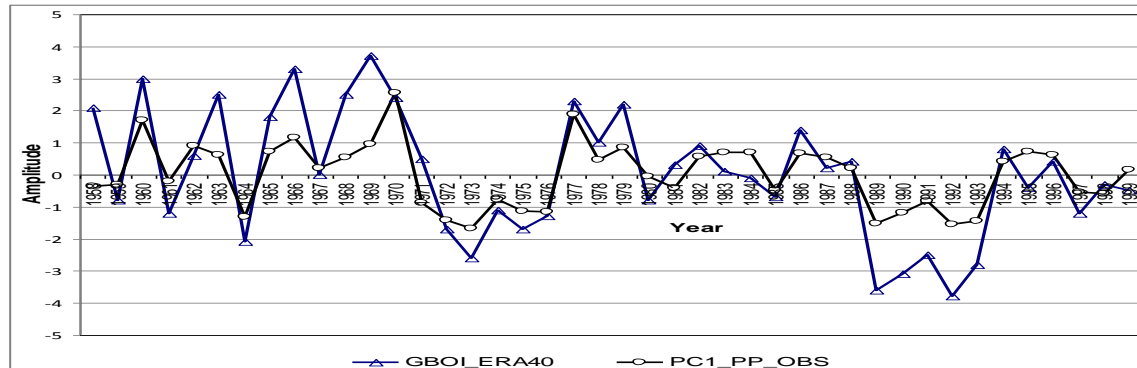
Table 3. Same as Table 2 but for 53 years (1948-2000).

Variable	Season	r	t	$\tau$	p	$N_{\text{eff}}$	CL
Correlation with aa							
<b>EBI (UF)</b>	<b>Spring</b>	<b>0.259</b>	<b>1.836</b>	<b>0.151</b>	<b>0.110</b>	<b>49</b>	<b>~95%</b>
<b>EBI (4-8)</b>	<b>Spring</b>	<b>0.528</b>	<b>3.864</b>	<b>0.382</b>	<b>0.000</b>	<b>41</b>	<b>&gt;99%</b>
ABI (UF)	Fall	-0.257	1.848	-0.118	0.210	51	~95%
ABI (9-15)	Spring	0.605	2.157	0.426	0.000	10	>95%
AEBI (9-15)	Winter	0.749	3.134	0.589	0.000	10	98.5%
Correlation with flux 10.7 cm							
TPPI(LPF)	Spring	0.444	1.502	0.322	0.001	11	85-90%
ABI(4-8)	Fall	0.578	4.124	0.312	0.001	36	99.9%
AEBI(4-8)	Fall	0.530	3.697	0.360	0.000	37	99.9%
<b>EBI (4-8)</b>	<b>Winter</b>	<b>0.419</b>	<b>2.678</b>	<b>0.272</b>	<b>0.004</b>	<b>37</b>	<b>98.5%</b>
Q_ORS(4-8)	Winter	-0.603	4.390	-0.351	0.000	36	99.9%
GBOI (4-8)	Winter	-0.695	6.034	-0.428	0.000	41	99.9%

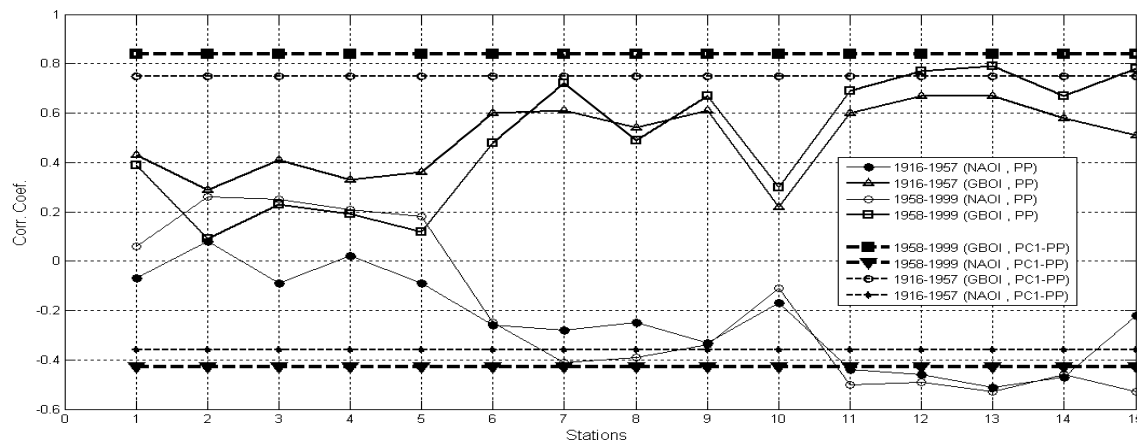
820  
821822  
823**Figure 1.** Localization of 15 precipitation stations situated upstream of Orsova station.



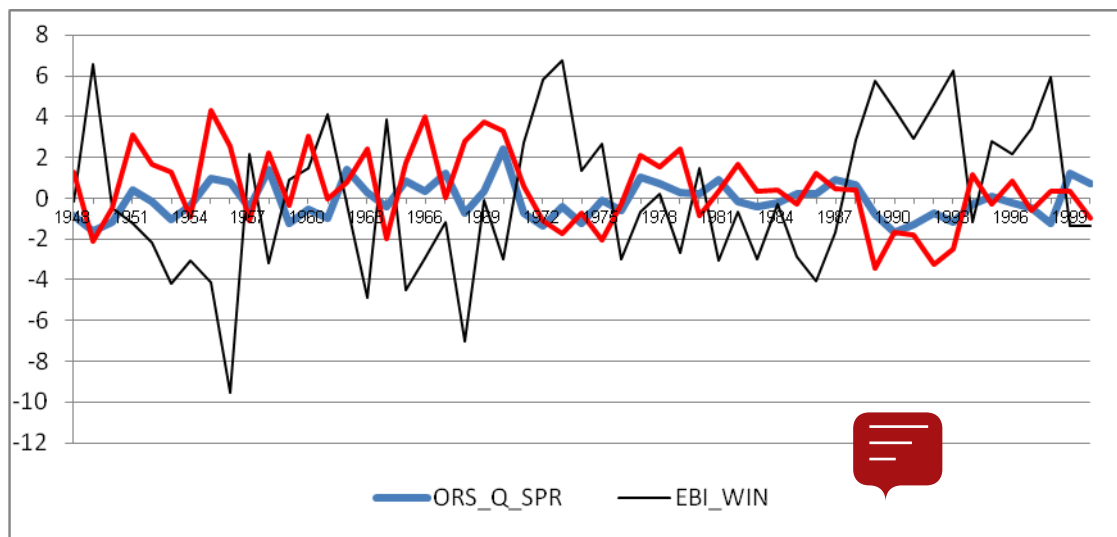
824  
825 **Figure 2.** Spatial distribution of correlation coefficients between SLP NCAR  
826 and observed PC1- PP during winter for 1958-1999.  
827  
828  
829



830 **Figure 3.** Winter precipitation PC1 versus winter GBOI for 1958-1999 ( $R=0.84$ ).  
831  
832  
833



834 **Figure 4.** Correlation coefficients between winter precipitation at 15 stations and NAOI and GBOI for  
835 two periods: a) 1916-1957; b) 1958-1999. The correlations between PC1-PP and two indices are  
836 marked by horizontal lines.  
837

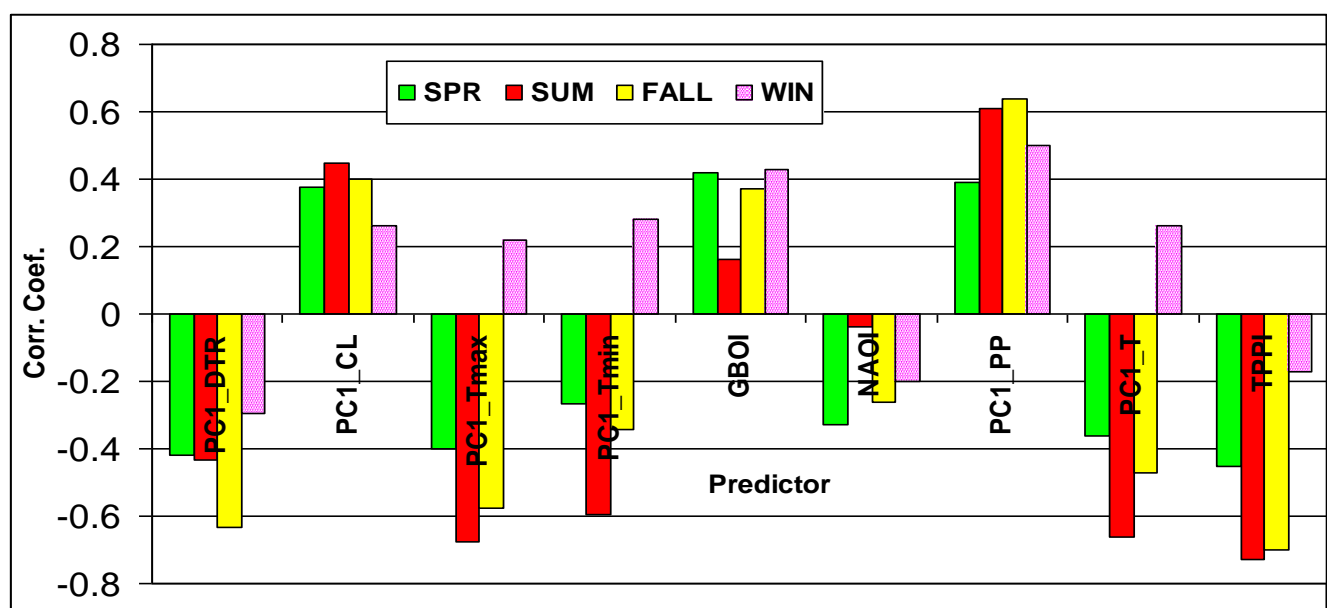
838  
839840 **Figure 5.** Spring Orsova discharge versus winter European blocking index ( $R = -0.54$ )  
841 and winter GBOI ( $R=0.53$ ) for the period 1948-2000.

842

843

844

845



846

847

848

849

850

848 **Figure 6.** Simultaneous correlations between Danube discharge at Orsova and nine predictors  
849 (1901-2000)

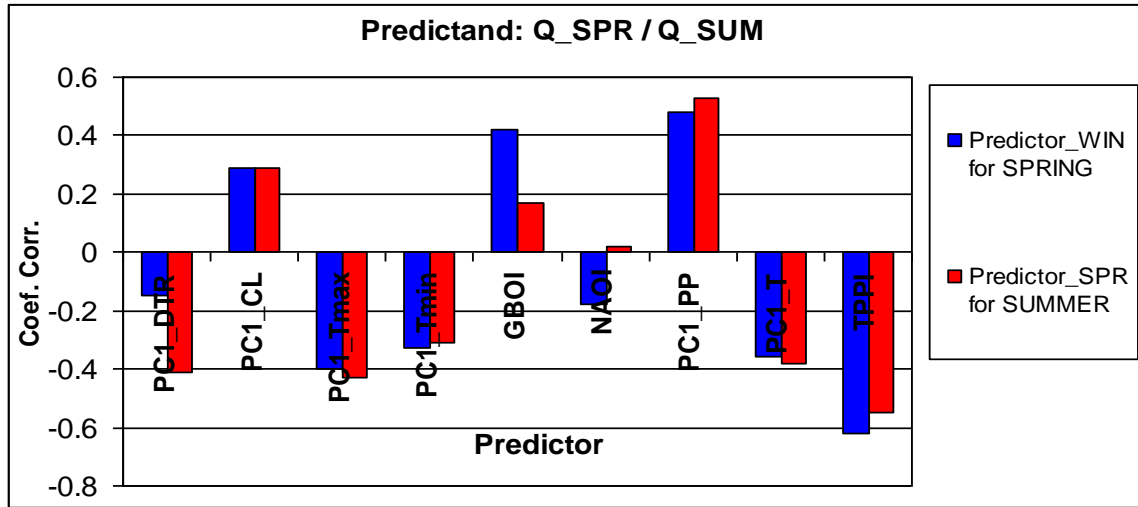
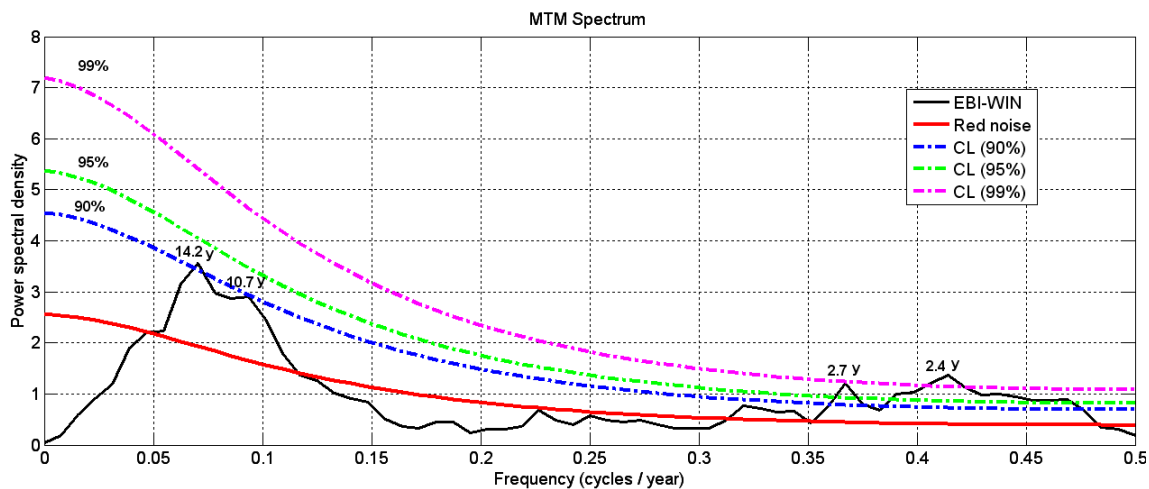
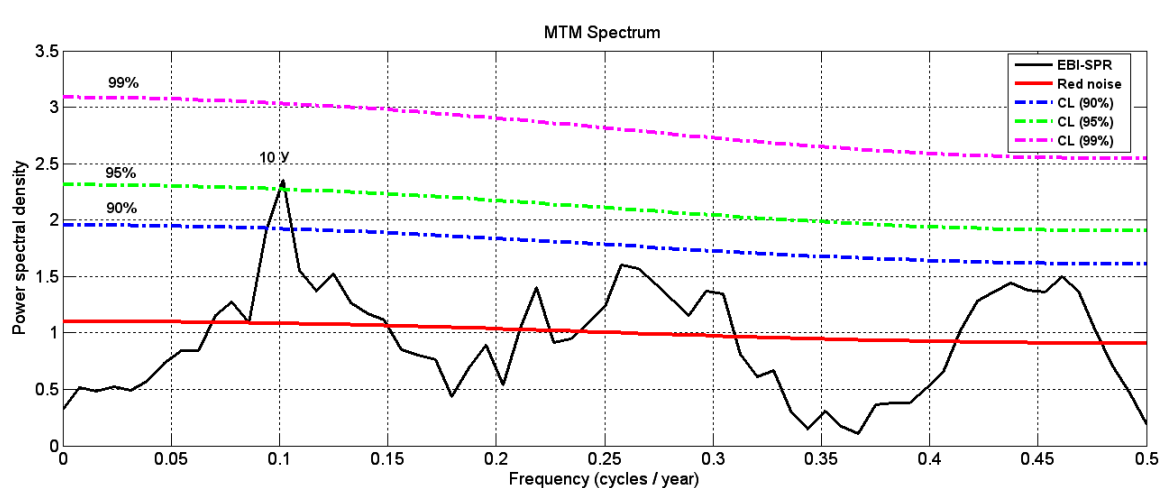


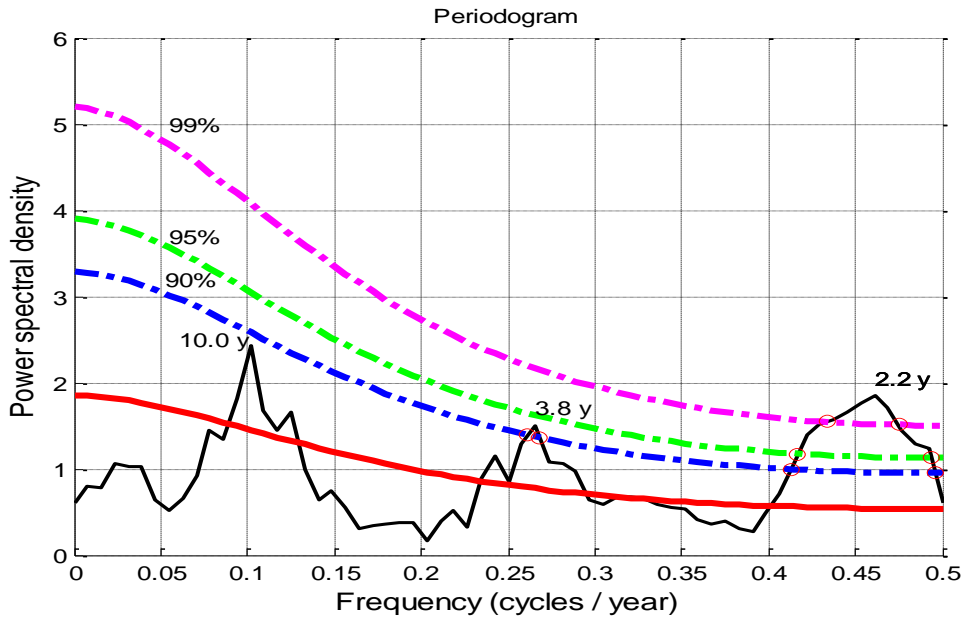
Figure 7. The correlation between Orsova discharge (Q) in the spring / summer and the nine predictors in the winter/spring.



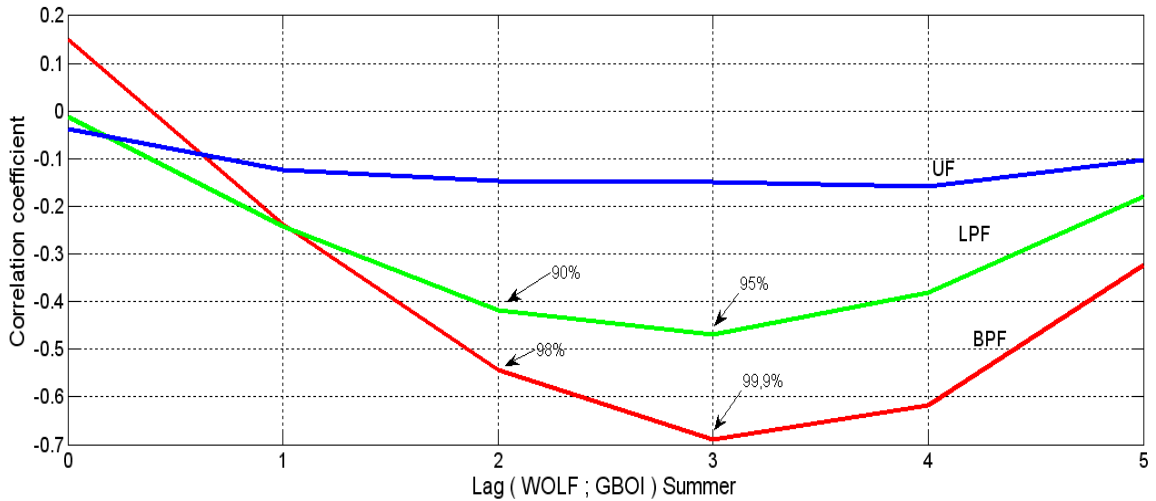
a)



b)



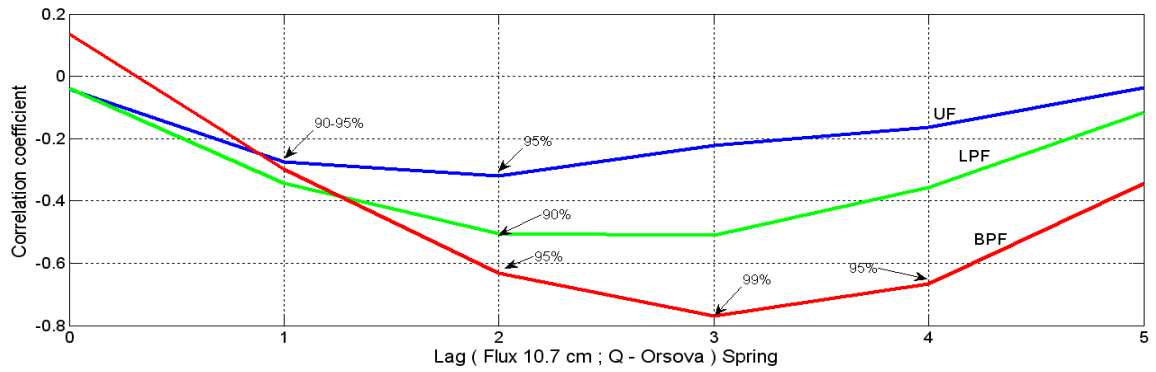
863  
864      c)  
865 **Figure 8.** Power spectra for the blocking indices: winter EBI (a),  
866 spring EBI (b)  
867 and spring AEBI (c).  
868  
869



870  
871  
872  
873 **Figure 9.** Correlation coefficients, between Wolf number and GBOI index in summer with  
874 the lags 0-5, for three time series: unfiltered (UF), smoothing by low pass filter (LPF) and by  
875 band pass filter (9-15)

876  
877  
878  
879  
880  
881  
882  
883  
884

885

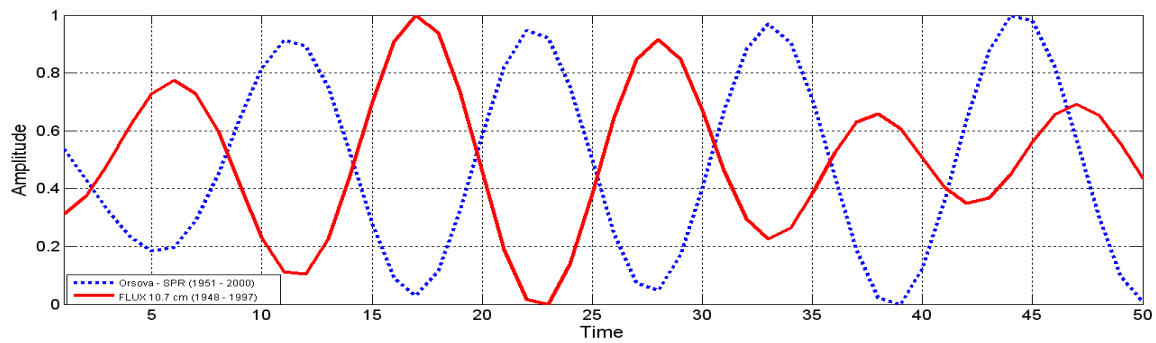


886

887

888

a)



889

890

**Figure 10.** Solar (Flux 10.7cm) signal in the Orsova discharge (Q\_ORS), during spring (1948-2000).

- a) Correlation coefficients, between solar flux and Orsova discharge with the lags 0-5, for three time series: unfiltered (UF), smoothing by low pass filter (LPF) and by band pass filter (9-15);
- b) Temporal behavior of the solar flux and Q\_ORS, filtered (9-15) with a delay of 3 years to flux. The time series are normalized.

891

892

893

894

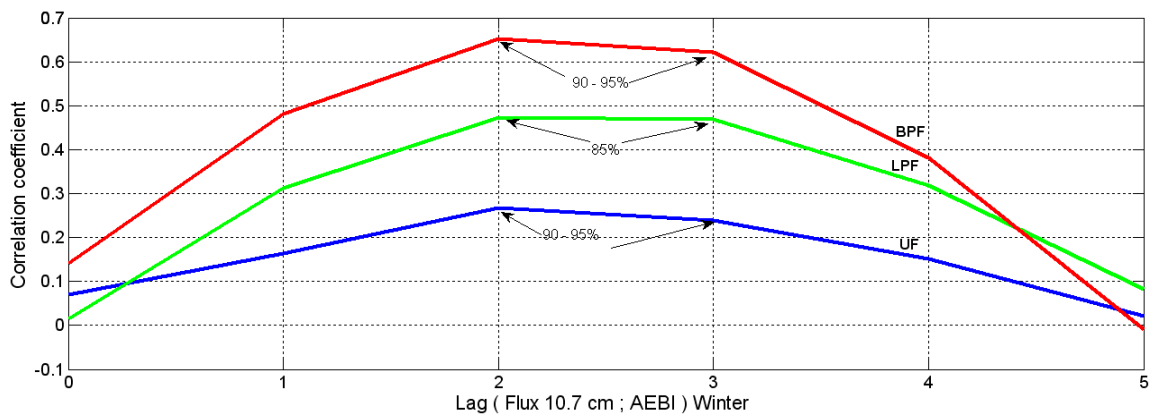
895

896

897

898

899



900

901

902

903

904

905

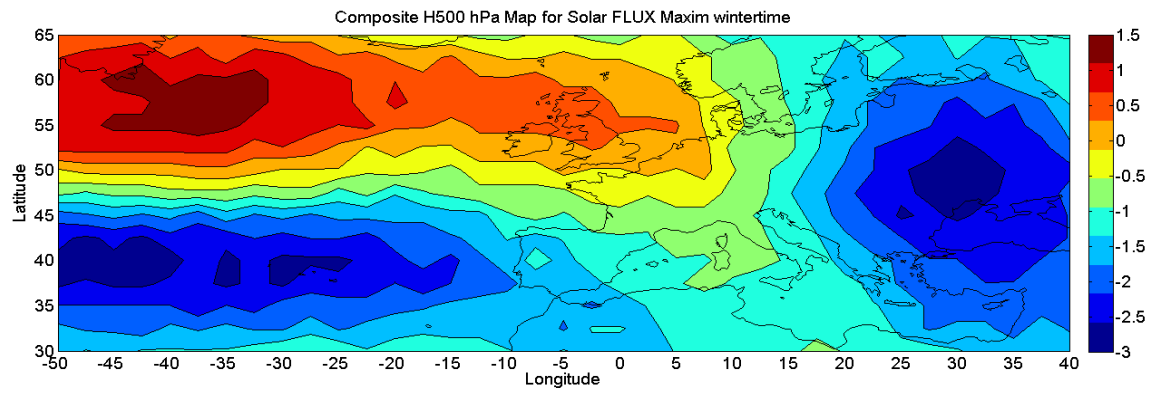
906

907

908

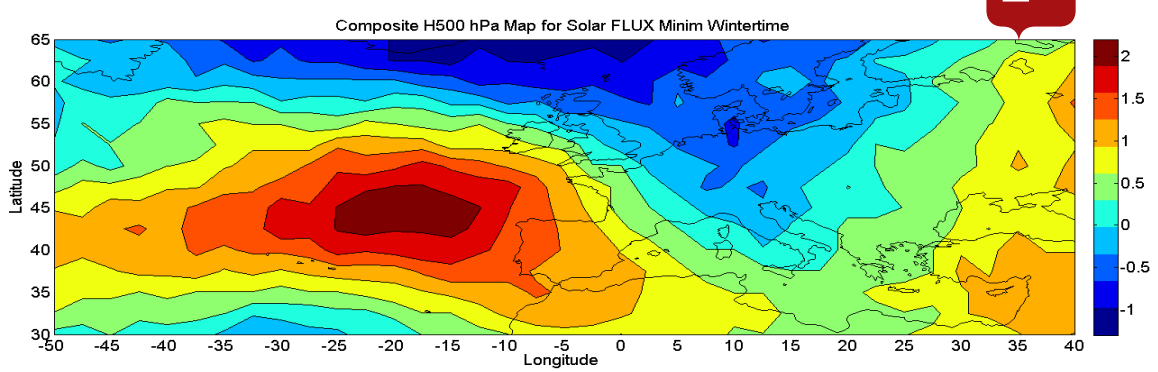
**Figure 11.** Correlation coefficients, between solar flux and AEBI with the lags 0-5, during winter (1948-2000), for three time series: unfiltered (UF), smoothing by low pass filter (LPF) and by band pass filter (9-15).

909



910

a)



b)

913

914

915

916

**Figure 12.** Composite maps for the winter H500 hPa anomalies, corresponding to solar flux associated with the east phase of QBO (1948-2000) and: a) maximum flux b) minimum flux

917

918